

Quenched Disorder Effects in Electron Transport in Si Inversion Layers in the Dilute Regime

V. M. Pudalov¹⁾²⁾, M. E. Gershenson⁺, N. N. Klimov^{+*}, H. Kojima⁺

P. N. Lebedev Physics Institute RAS, 119991 Moscow, Russia

⁺*Department of Physics and Astronomy, Rutgers University, New Jersey 08854, USA*

^{*}*P. N. Lebedev Physics Research Center, 119991 Moscow, Russia*

Submitted 21 July 2005

In order to reveal the effects of disorder in the vicinity of the apparent metal-insulator transition in 2D, we studied the electron transport in the same Si- device after cooling it down to 4 K at different fixed values of the gate voltage V^{cool} . Different V^{cool} did not modify significantly either the momentum relaxation rate or the strength of electron-electron interactions. However, the temperature dependences of the resistance and the magnetoresistance in parallel magnetic fields, in the vicinity of the 2D metal-insulator transition, carry a strong imprint of the quenched disorder determined by V^{cool} . This demonstrates that the observed transition between metallic and insulating regimes, besides universal effects of electron-electron interaction, depends on a sample-specific localized states (disorder). We report an evidence for a weak exchange in electrons between the reservoirs of extended and resonant localized states which occur at low densities. The strong cool-down dependent variations of $\rho(T)$, we believe, are evidence for developing spatially inhomogeneous state in the critical regime.

PACS: 71.27.+a, 71.30.+h, 72.20.Ee, 73.40.Qv

After about a decade of intensive research, the apparent metal-insulator transition (MIT) in two-dimensional (2D) systems remains a rapidly evolving field [1]. One of the central problems here is to understand individual roles of two major driving forces, disorder and electron-electron (e-e) interactions. A great body of experimental data demonstrates that, at sufficiently large carrier densities, the low-temperature behavior of disordered systems is governed by the universal quantum interaction corrections to the conductivity [2–4]. These purely interaction effects between mobile 2D electrons have been intensively studied both theoretically [2–8] and experimentally [9–13]; the role of disorder in these studies is limited to scattering of mobile electrons solely.

In contrast, the interplay of disorder and interactions, particularly, interaction between localized and mobile electrons is considered much rarely [14–18]. There are clear observations that near the apparent 2D MIT, the behavior of dilute systems is very rich, and does not necessarily follow the same pattern [18–20]. One might expect that the interplay of the disorder and interactions should become more and more important as electron density decreases and approaches the critical density of the 2D MIT.

Usually, the presence of the localized states itself in 2D transport is masked by mobile electrons. In order to reveal their contribution in the vicinity of the 2D MIT, we have studied the electron transport in the same Si-MOS structure, which was slowly cooled down from room temperature to $T = 4\text{ K}$ at different fixed values of the gate voltage $V_g = V^{\text{cool}}$. Changing the cooling conditions affects primarily the thickness of the potential well [21]. We believe that this allowed us to vary fine details of disorder – the structure of the resonant (localized) states – without affecting the type of disorder (short-ranged), the scattering rate, and the strength of electron-electron interactions in the system of mobile electrons. We focused on two key features of the 2D MIT, strong dependences of the resistivity on the temperature and parallel magnetic field, and studied them in the density range $n = (0.7–3) \cdot 10^{11} \text{ cm}^{-2}$ for a system with a snapshot disorder pattern.

We have observed that at relatively high densities (resistivity $\rho \leq 0.1h/e^2$), the dependences $\rho(T)$ and $\rho(B_{\parallel})$ in weak parallel magnetic fields B_{\parallel} are very similar for different cooldowns. This “universal” behavior of transport at high densities agrees with our observation [11] of the sample-independent $\rho(T\tau, n)$ for samples with different mobility ($\mu \propto \tau$). In contrast, at low densities ($\rho \sim (0.1–1)h/e^2$), or in moderate and strong parallel fields $g\mu_B B_{\parallel} \sim E_F \gg k_B T$, the cooling conditions affect dramatically the transport even though the main para-

¹⁾ Член редколлегии “Писем в ЖЭТФ” с 2000 г. по настоящее время.

²⁾ e-mail: pudalov@Mail1.lebedev.ru

meters of disorder and of electron interactions remain unchanged. This observation provides direct experimental evidence that near the 2D MIT the electron transport at finite temperatures in dilute systems becomes sample-specific and dependent on more subtle details of disorder.

We have also observed that the frequency of the weak-field Shubnikov-de Haas (SdH) oscillations varies with temperature and in-plane field; these variations (of the order of a few %) grow as density approaches the 2D MIT critical density. The SdH-frequency is directly related with the density of mobile electrons, whatever strong interactions are. Therefore, the observed variations of the mobile charge at a fixed total charge in the MOS-capacitor evidence for the redistribution of electrons between the bands of mobile and localized states. The weak T -dependence of this electron exchange, if attributed to activation processes, indicates the presence of very low energy barriers (~ 1 K) between the mobile and localized electron states. We relate the finite temperature cool-down effects to the hybridization of the mobile and spatially separated resonant (localized) states present at the Fermi energy at low densities.

The resistivity measurements were performed on a high mobility Si-MOSFET sample [22] at the bath temperatures 0.05–1.2 K. The crossed magnetic field system allowed to accurately align the magnetic field parallel to the plane of the 2D electron system [9]. Five different cool-down were done with $V^{\text{cool}} = 0, 5, 10, 18,$ and 25 V. The carrier density, found from the period of SdH oscillations, varies linearly with V_g : $n \approx C \times (V_g - V_{\text{th}})$, where $C (= 1.10 \cdot 10^{11} / \text{Vcm}^2$ for the studied sample) is determined by the oxide thickness. The threshold voltage V_{th} varied little (within 0.15 V) for different cool-downs and remained fixed as long as the sample was maintained at low temperatures (up to a few months). Within the same cool-down, both C and V_{th} remained constant (within a few %) overall studied range of densities.

Fig.1 shows the mobility μ versus V_g for five different cool-downs with $V^{\text{cool}} = 0, 5, 10, 18,$ and 25 V. The peak mobility for different V^{cool} varies by less than $\sim 7\%$; this demonstrates that the momentum relaxation time τ is not strongly affected by the cooling conditions. Comparing the $\mu(n)$ curves with the conventional transport theory [23, 24], we conclude that the density of charged impurities varies by less than $1 \cdot 10^{10} \text{cm}^{-2}$ for different cool-downs. We also observed that the amplitudes of the SdH oscillations are similar for different cool-downs, as shown in the inset to Fig.1. These two observations are consistent with each other, since the quantum lifetime τ_q is nearly equal to τ for Si-MOSFETs.

Fig.2 shows that the $\rho(T)$ dependences are cooldown-independent far from the transition (at $\rho \ll h/e^2$) (see,

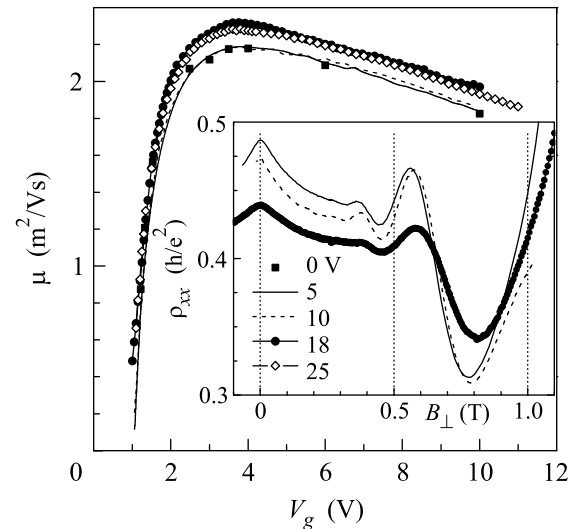


Fig.1. The mobility versus the gate voltage for different cool-downs. The V^{cool} values for both the main panel and the inset are shown in the figure. Examples of the SdH oscillations, shown in the inset for the same $V_g = 1.15$ V, $T = 0.1$ K, $B_{\parallel} = 0.03$ T, demonstrate that the quantum time τ_q is not very sensitive to the cooling conditions. Carrier densities vary within the interval $(1.07-1.09) \cdot 10^{11} \text{cm}^{-2}$

e.g., curves 9, 10). However, in the vicinity of the transition ($\rho \sim h/e^2$), a dramatically different behavior is observed as temperature increases. The irreproducibility of $\rho(T)$ for different cool-downs is clearly seen for the curves in Fig.2 which correspond to nearly the same ρ at the lowest T : these curves, being different at higher temperatures, converge with decreasing T . We have verified that the renormalization of electron spin susceptibility and effective mass (and thus the two Fermi-liquid coupling constants) do not change for different cool-downs, to within 5%. Thus, the electron-electron interaction effects [11] also can not be accounted for the changes in $\rho(T)$.

The sample-specific variations vanish at sufficiently low temperatures: this suggests that the underlying mechanism is related to the finite-temperature effects in a system which retains a quenched disorder. These results also suggest that, in addition to universal effects, a finite-temperature and sample-specific mechanism, which strongly affects the resistivity, comes into play.

If the behavior shown in Fig.2 is characterized by a critical density n_c , which corresponds to the transition, the latter would have been cooldown-dependent. The labels in Fig.2 mark two $\rho(T)$ dependences, which corresponded to $n = n_c$ for two different cool-downs; they were estimated from linear extrapolation to zero of the activation energy $\Delta(n)$ measured in the insu-

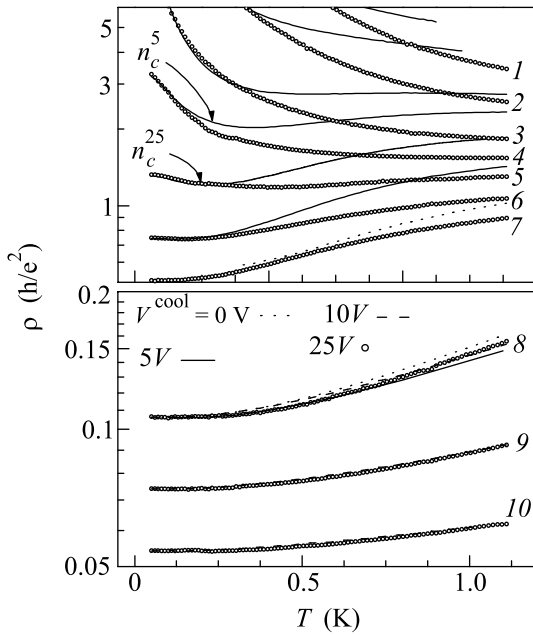


Fig.2. Temperature dependences of the resistivity for four different cool-downs. For curves 1 to 10, the density values are 0.827, 0.882, 0.942, 0.972, 1.00, 1.038, 1.07, 1.18, 1.31, 1.53, in unites of 10^{11} cm^{-2} . n_c^5 and n_c^{25} mark two critical dependences for cooldowns at $V_g = 5$ and 25 V , respectively

lating regime $\rho(T) \propto \exp(\Delta/T)$ [20, 25], away of the critical regime. It is clear that the critical dependences $\rho(T, n = n_c)$ are non-monotonic (see also Refs. [25, 26]). The non-monotonicity is not caused by electron overheating; we applied sufficiently low source-drain current in order to reduce the excess in electron temperature δT_e to a few mK. For example, for the curve “ n_c^{25} ” (the source, drain resistance 150 kOhm each, channel resistance $\sim 30 \text{ kOhm}/\square$) the chosen source-drain excitation $10 \mu\text{V}$ corresponds to dissipation $\sim 10^{-15} \text{ W}$ which might cause electron overheating $\lesssim 1 \text{ mK}$ [26].

Since the cooldown-dependent changes in $\rho(T)$ vanish with temperature decreasing, we have attempted to analyze the variations $\delta\rho(T) = \rho(V_1^{\text{cool}}, T) - \rho(V_2^{\text{cool}}, T)$ in terms of the exponential $\exp(-\Delta/T)$ dependence, as demonstrated in Fig.3. The corresponding “activation” energy Δ is very low: it varies within the interval $\sim (0.7-1) \text{ K}$. This proves that the low-lying band of localized states (located close to the bottom of the conduction band, $\approx 8 \text{ K}$ below the Fermi level) is irrelevant. The smallness of Δ , therefore, points at the involvement of the localized states which are located close to the Fermi level. Similar resonant localized states are known in the narrow band-gap semiconductors and must be spatially separated from the mobile states.

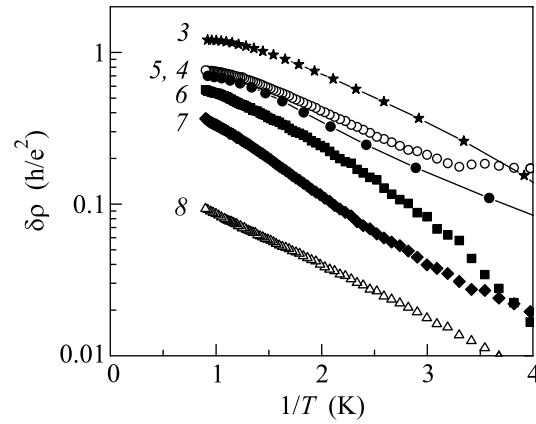


Fig.3. Difference between resistivity values for two different cool-downs (shown in Fig.2) versus inverse temperature. The numbers label the curves for densities same as in Fig.2

We now turn to the magnetoresistance (MR) in parallel fields; the data are shown in Figs.4 and 5. This MR which is usually associated with the spin effects [1, 19].

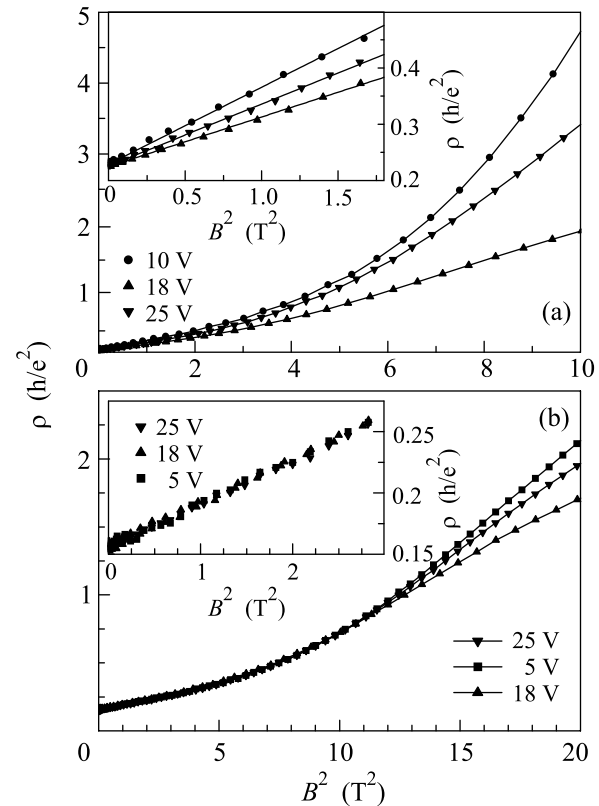


Fig.4. Examples of the dependences $\rho(B_{\parallel}^2)$ at $T = 0.3 \text{ K}$ for the carrier density (a) $1.20 \cdot 10^{11} \text{ cm}^{-2}$ and (b) $1.34 \cdot 10^{11} \text{ cm}^{-2}$. The insets blow up the low-field region of the quadratic behavior. The values of V^{cool} are indicated for each curve

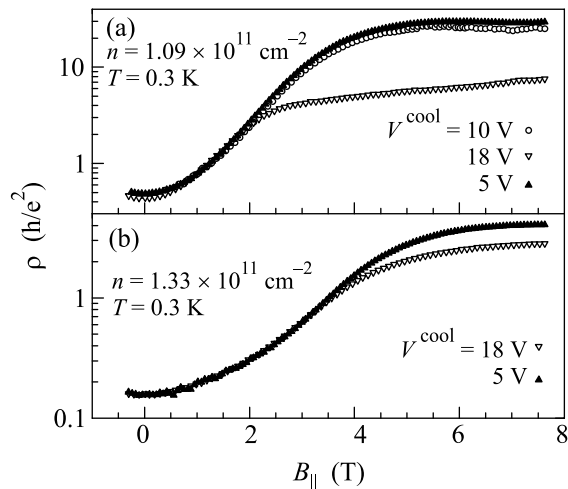


Fig.5. Resistivity vs B_{\parallel} -field for three cool-downs at two electron densities

In the theoretical models of the parallel-field MR, based on electron-electron interactions, the MR is controlled by the effective g^* -factor and the momentum relaxation time τ [6, 11, 4]. An important advantage of our method is that as we mentioned above, cooling of the same sample at different V^{cool} does not affect these parameters. Thus, one might expect to observe a sample-independent behavior if the MR is controlled solely by the universal interaction effects.

Firstly, we consider the range of fields much weaker than the field of complete spin polarization ($g^*\mu_B B_{\parallel} \ll E_F$). The insets to Figs.4a and 4b show that the MR is proportional to B_{\parallel}^2 at $g^*\mu_B B_{\parallel}/k_B T \leq 1$. We found that the slope $d\rho/dB^2$ is nearly cooldown-independent (i.e. universal) only for the densities $n > 1.3 \cdot 10^{11} \text{cm}^{-2}$ (which are by 30% greater than the critical density n_c), or for the resistivities $\rho(0) < 0.16h/e^2$ (compare insets to Figs.4a and 4b); this is consistent with our earlier observations [11]. With approaching n_c , this universality vanishes: Figure 4 a shows that even when the zero-field resistivity is as small as $0.22h/e^2$, the slope varies by a factor of 1.3 for different V^{cool} .

For the intermediate fields, $k_B T < g^*\mu_B B_{\parallel} < E_F$, the $\rho(B_{\parallel})$ behavior is not universal over the whole density range $n = (1-3) \cdot 10^{11} \text{cm}^{-2}$ (Figs.4). As n decreases and approaches n_c , the cooldown-dependent variations of $\rho(B_{\parallel})$ increase progressively.

The influence of cool-down conditions to the magnetoresistance becomes even more dramatic in strong fields, $B_{\parallel} \gtrsim E_F/g^*\mu_B$. Despite the fact that the dependences $\mu(n) \propto \tau(n)$ for different cool-downs are very similar (Fig.1), we observed very large variations in the high-field MR. Figs.5a,b show $\rho(B_{\parallel})$ for different cool-downs at two values of n . The cooldown conditions

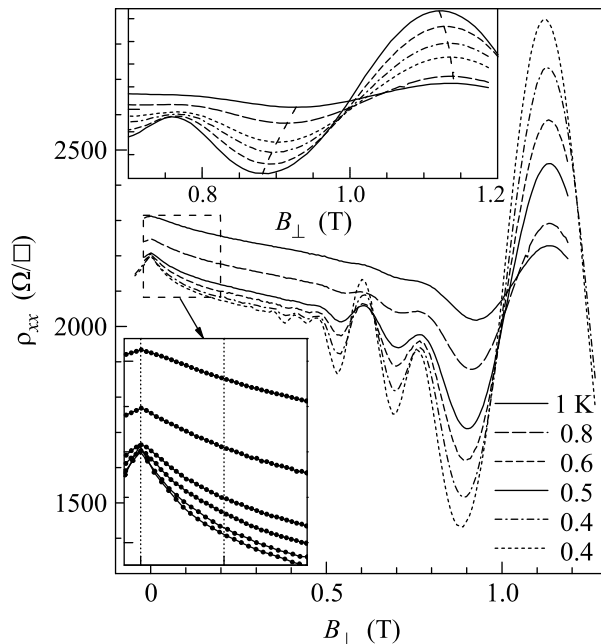


Fig.6. Typical Shubnikov-de Haas oscillations at six temperatures (indicated on the main panel) and in-plane field $B_{\parallel} = 0.02 \text{ T}$. Nominal density value $n \approx 2 \cdot 10^{11} \text{cm}^{-2}$. The lower left inset demonstrate precise control of the zero magnetic field position, the upper inset magnifies one of the oscillations to show its shifting with T

cause factor-of-five changes in $\rho(B)$ in high fields and factor-of-two changes in the values of $B_{\parallel} = B_{\text{sat}}$ at which the MR “saturates” at a given carrier density. The latter quantity was determined from the intercept of the tangents at fields below and above MR saturation [19].

The non-universal, sample-dependent behavior of $\rho(B_{\parallel})$ agrees with earlier observations made on different samples [19]. We emphasize that the curves for different V^{cool} (in each of Figs.5a,b) correspond to nominally the same density. The fact that B_{sat} is a cooldown-dependent parameter, proves that the MR in strong parallel fields is not solely related to spin-polarization of mobile electrons. The fact that the variations arise in strong fields $g\mu_B B_{\parallel} \sim E_F$ hints that a deep tail of localized states located near the bottom of the conduction band (or near the bottom of the upper spin-subband) [14, 15, 27, 28] is responsible for the magnetoresistance variations. We note, that at low temperatures $T = 0 - 1 \text{ K} \ll T_F$ and at zero field, the temperature activation of carriers from the tail of localized states to the Fermi level (across the energy gap $\sim E_F$) is negligibly weak and could not affect the data shown in Fig.2. In contrast, at higher temperatures $T \sim T_F$, the thermal activation of carriers from the tail of localized states to the Fermi level produces noticeable effects, detected in to the Hall voltage [29].

It is worth mentioning that the influence of variable disorder on transport and magnetotransport in Si-MOSFETs has been studied earlier. Both the temperature dependence $\rho(T)$ and magnetoresistance $\rho(B_{\parallel})$ were found to be different in samples with different mobility [20, 19], in samples cooled down with different values of substrate bias voltage [30], and with intentionally varied oxide charge [23]. In contrast, in our studies we kept constant the scattering time, quantum time, phase breaking time, interface charge and parameters relevant to electron-electron interaction. Even under such conditions, the strong non-universal variations in $\rho(T)$ and $\rho(B_{\parallel})$ occur.

In order to elucidate the origin of the observed variations in disorder, we have analyzed SdH-oscillations at weak perpendicular magnetic fields versus temperature and in-plane magnetic field. Figure 6 shows typical $\rho_{xx}(B_{\perp})$ curves for six temperatures, measured during the same cooldown, for a fixed gate voltage value. The ρ_{xx} minima occur when the Fermi energy coincides with the middle of the energy gap. The upper-left inset clearly shows that the minima of the oscillations shift with temperature, thereby evidencing for the changes in the density of mobile carriers. The lower-left inset demonstrates that the shift of the ρ_{xx} minima is not caused by variations in the residual field of the superconducting magnet (maintained at 4 K).

We fitted the total oscillatory picture with theoretical dependence (similar to that in Ref. [9]), using the frequency of oscillations n_{SdH} for each curves as fitting parameter. The resulting temperature dependences of n_{SdH} are shown in Fig.7. The error bars on the figure correspond to relative changes of the frequency with temperature; the absolute frequencies are determined with about three times lower precision. At higher density $n > 5 \cdot 10^{11} \text{ cm}^{-2}$ the oscillation frequency was independent of temperature, within the 0.5% uncertainty. The $n_{\text{SdH}}(T)$ changes become noticeable at frequency $\leq 4 \cdot 10^{11} \text{ cm}^{-2}$ (which is four times larger than the critical density of the 2D MIT); they increase progressively with the in-plane field, as Figs.7a and b show.

Discussion. The measured density values n_{SdH} refer to the density of mobile electrons which participate in the Landau quantization. Weak temperature variations of the density of mobile electrons do not involve large energy scale of the order of $E_F \sim 8 \text{ K}$. This points at the presence of the resonant localized states at the Fermi level, separated spatially and by a small energy barrier from the mobile states. The density variations then are caused by exchange in electrons between those two states via either overbarrier transitions as schematically drawn in Fig.7, or via tunnelling.

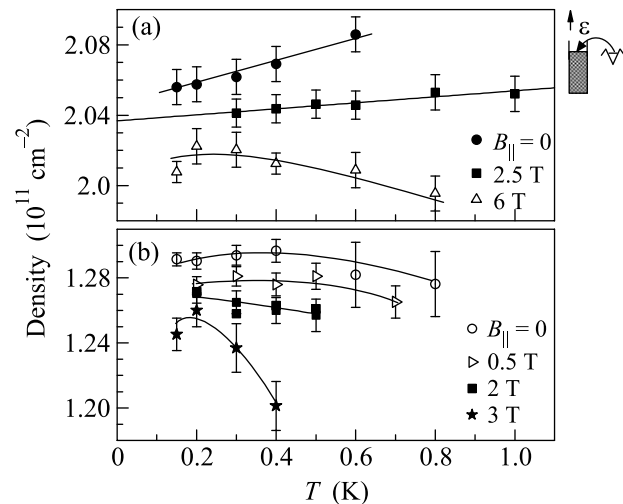


Fig.7. Temperature dependences of the frequency of SdH oscillations at two fixed values of the gate voltage. Different curves within each panels are offset shifted, for clarity. Diagrams on the right show schematically DOS for the band of mobile electrons and a resonant state. The arrow shows an overbarrier transition

The temperature induced exchange in electrons between the bands of mobile and localized states, by itself, can not produce significant effect on the resistivity. Indeed, the appearance (disappearance) of $\sim 10^9 \text{ cm}^{-2}$ charged scatterers (which corresponds to the 0.5% variations of density in Fig. 7) may cause, correspondingly, 0.5% changes in ρ . However, in the critical regime, the localized states may be expected to occupy a significant share of the total 2D layer by forming clusters. The periphery of the cluster is expected to consist of the resonant states which may emit and absorb electrons. As a result, the overall area available for motion of mobile electrons changes with temperature, similar to that in the known percolation picture [31]. The resonant states thus may control transport through the saddle-points separating neighboring areas occupied by mobile electrons, and thus, indirectly trigger the strong changes in ρ .

In the B_{\parallel} field, the resonant state should split and move relative the band of mobile states. This model may potentially explain both, strong variations of $\rho(T)$ and $\rho(B_{\parallel})$ in the critical regime, and weak changes of the mobile carrier density. Formation of the two-phase state may be caused by either disorder or electron-electron interactions. Spontaneous formation of the heterophase state in the vicinity of the phase transition was established for quasi-1D system [32]; in 2D electron system, the two-phase state is also intrinsic to some theoretical models [33].

To summarize, by cooling the same high-mobility Si-MOS sample at different fixed values of the gate voltage, we tested universality of the temperature and magnetic-field dependences of the resistivity near the 2D MIT. An important advantage of this approach is that the different cooldown procedures do not alter the interactions effects between mobile carriers. It has been found that in the vicinity of the transition ($\rho \sim h/e^2$), the cooldown-specific effects strongly affect $\rho(T)$; these effects vanish only when ρ decreases below $\sim 0.1h/e^2$ with increasing electron density; they also vanish as T decreases. The non-universal behavior is especially dramatic in strong B_{\parallel} fields where it extends to much higher electron densities (we observed pronounced non-universality of $R(B_{\parallel})$ over a range $n = (1 - 3) \cdot 10^{11} \text{ cm}^{-2}$).

Our results reveal the existence of the resonant (shallow) localized states near the Fermi energy. The observed temperature variation of the frequency of Shubnikov-de Haas oscillations demonstrates a weak exchange in electrons between the reservoirs of mobile and resonant localized states. The large changes of $\rho(T)$ at elevated temperature signify the development of a spatial inhomogeneity of the 2D system, which may result from either interactions between electrons or disorder.

One of the authors (VP) acknowledges discussions with V. I. Kozub and Yu. M. Galperin. The work was supported by the NSF, RFBR, Programs of the Presidium and of the Division of Physical Sciences of RAS, and the Presidential Program "The State Support of Leading Scientific Schools".

1. E. Abrahams, S. Kravchenko, and M. P. Sarachik, *Rev. Mod. Phys.* **73**, 251 (2001).
2. For a review, see: B. L. Altshuler and A. G. Aronov, in *Electron-electron interactions in disordered systems*, Eds. A. L. Efros and M. Pollak, Elsevier, Amsterdam, 1985. P. A. Lee and T. V. Ramakrishnan, *Rev. Mod. Phys.* **57**, 287 (1985).
3. G. Zala, B. N. Narozny, and I. L. Aleiner, *Phys. Rev. B* **64**, 214204 (2001); *ibid.* **65**, 20201R (2002).
4. I. V. Gornyi and A. D. Mirlin, *Phys. Rev. B* **69**, 045313 (2004).
5. S. Das Sarma and E. H. Hwang, *Phys. Rev. Lett.* **83**, 164 (1999).
6. A. M. Finkelstein, *Sov. Sci. Reviews/section A-Physics Reviews*, Ed. I. M. Khalatnikov, **14**, 3 (1990).
7. C. Castellani, C. Di Castro, P. A. Lee, and M. Ma, *Phys. Rev. B* **30**, 527 (1984); C. Castellani, G. Kotliar, and P. A. Lee, *Phys. Rev. Lett.* **59**, 323 (1987); C. Castellani, C. Di Castro, H. Fakuyama et al., *Phys. Rev. B* **33**, 7277 (1986); C. Castellani, C. Di Castro, and P. A. Lee, *ibid.* **57**, R9381 (1998).
8. A. Punnoose and A. M. Finkelstein, *Phys. Rev. Lett.* **88**, 016802 (2002).
9. V. M. Pudalov, M. Gershenson, H. Kojima et al., *Phys. Rev. Lett.* **88**, 196404 (2002).
10. Y. Y. Proskuryakov, A. K. Savchenko, S. S. Safonov et al., *Phys. Rev. Lett.* **89**, 076406 (2002).
11. V. M. Pudalov, M. Gershenson, H. Kojima et al., *Phys. Rev. Lett.* **91**, 126403 (2003).
12. S. A. Vitkalov, K. James, B. N. Narozhny et al., *Phys. Rev. B* **67**, 113310 (2003).
13. J. Zhu, H. L. Stormer, L. N. Pfeiffer et al., *Phys. Rev. Lett.* **90**, 056805 (2003).
14. N. F. Mott, *Metal-Insulator Transitions*, Taylor and Francis Ltd., London, 1974.
15. V. I. Kozub and N. V. Agrinskaya, *Phys. Rev. B* **64**, 245103 (2001).
16. T. M. Klapwijk and S. Das Sarma, *Sol. St. Commun.* **110**, 581 (1999).
17. B. L. Altshuler and D. L. Maslov, *Phys. Rev. Lett.* **83**, 2092 (1999).
18. V. M. Pudalov, G. Brunthaler, A. Prinz, and G. Bauer, *cond-mat/0103087*.
19. V. M. Pudalov, G. Brunthaler, A. Prinz, and G. Bauer, *Phys. Rev. Lett.* **88**, 076401 (2002).
20. V. M. Pudalov, G. Brunthaler, A. Prinz, and G. Bauer, *JETP Lett.* **68**, 442 (1998).
21. V^{cool} determines the depth of the confining potential well and, simultaneously, the number of interface traps sunk under the Fermi level. At low temperatures, as V_g is varied, the potential well remains almost unchanged and memorizes an imprint of the disorder formed during its cooling down.
22. Sample Si6-14 with 190 nm thick gate oxide was fabricated on (001)-Si wafer and had a rectangular channel 2.5×0.25 mm oriented along [010].
23. For a review see, T. Ando, A. B. Fowler, and F. Stern, *Rev. Mod. Phys.* **54** (2) (1982).
24. A. Gold and W. Götze, *Phys. Rev. B* **33**, 2495 (1986).
25. B. L. Altshuler, D. L. Maslov, and V. M. Pudalov, *Physica E* **9**, 209 (2001).
26. O. Prus, M. Reznikov, U. Sivan, and V. Pudalov, *Phys. Rev. Lett.* **88**, 016801 (2002).
27. S. A. Vitkalov, M. P. Sarachik, and T. M. Klapwijk, *Phys. Rev. B* **65**, 201106 (2002).
28. A. Gold and V. T. Dolgoplov, *Phys. Rev. Lett.* **89**, 129701 (2002).
29. A. Yu. Kuntsevich, D. A. Knyazev, V. I. Kozub et al., *Pis'ma ZhETF* **81**, 502 (2005) [*JETP Lett.*, **81**, 409 (2005)].
30. A. Lewalle, M. Pepper, C. J. B. Ford et al., *cond-mat/0108244*.
31. Y. Meir, *Phys. Rev. Lett.* **83**, 3506 (1999).
32. A. V. Kornilov, V. M. Pudalov, Y. Kitaoka et al., *Phys. Rev. B* **69**, 224404 (2004).
33. B. Spivak, *Phys. Rev. B* **64**, 085317 (2001).